DIESEL PARTICULATE FILTER LOADING AND REGENERATION ISSUES IN CITY/CONGESTED DRIVING

Xuereb. E. and Farrugia. M.
Department of Mechanical Engineering,
University of Malta,
Msida MSD 2080,
Malta
E-mail: emilio.xuereb.10@um.edu.mt and mario.a.farrugia@um.edu.mt

ABSTRACT

Diesel particulate filters (DPF) are a widely used after-treatment method adopted in current diesel engines and the Gasoline Particulate Filter (GPF) is in the pipeline for future gasoline direct injection. The DPF accumulates soot from normal engine running and is then expected to burn off the accumulated soot during regeneration instances. The regeneration instance can be both due to normal engine driving or is Engine Control Unit (ECU) assisted. In city or congested driving situations, the regeneration can be difficult to achieve. Such slow speed driving is also the case in a small island as Malta. Many people are experiencing DPF blockage problems which sometimes lead to undrivable vehicles.

The ECU monitors the level of loading mainly through the differential pressure sensor. This paper discusses soot loading models currently available in the literature and their performance vis-à-vis the actual soot loading level is analyzed. It was determined that different models lead to disagreement in predicted delta p. The widest discrepancy between models was of more than a factor of 10.

Physical weight measurement of soot loading from soot blocked DPFs was conducted by oxidation in a furnace. The residues leftover from the furnace regeneration were also analyzed and the soot/ash ratio was quantified. It was determined that the ash left is very low, meaning that the DPFs were blocked with soot and not ash. This was attributed to the inability to have regeneration of the DPF whilst driving to the very low speed low load driving conditions experienced in Malta.

INTRODUCTION

Diesel Particulate Filters (DPFs) have been used for decades and were made mandatory on all diesel powered vehicles for the last 10 years. This is attributed to the fact that European Emission Standards are becoming more stringent when dealing with Particulate Matter (PM) and Nitrogen Oxides (NO_x) emissions. Engine technology helps to reduce PM emissions but with the standards proposed for the Euro 5 & 6 vehicles, exhaust after treatment is needed to reduce the PM emissions below 0.005g/km[1].

Soot found in diesel exhaust is trapped into the honeycomb structure of the DPF and as the back pressure exceeds a pre-defined limit, the ECU (Engine Control Unit) trigger a regeneration process during which the accumulated soot is burnt off as Carbon Dioxide (CO_2)[2].

NOMENCLATURE

DPF		Diesel particulate Filter
DOC		Diesel Oxidation Catalyst
ECU		Engine Control Unit
d_{hs}	[m]	Hydraulic Diameter
D	[m]	Monolith Diameter
F	[-]	Factor 28.454
Fr	[-]	Friction Coefficient
k	[m^2]	Monolith wall Permeability
k_e	[m^2]	Thermal Conductivity
k_{soot}	[m^2]	Particulate Layer Permeability
K_f	[-]	Flow Correlation Factor for flow through DPF channel
L	[m]	Monolith Cell Length
$L_{filtration}$	[m]	Filtration Length
L_{plug}	[m]	Length of Plug
N	[-]	Number of Inlet Cells
Q	[m^3/s]	Exhaust Volumetric Rate
Re	[-]	Reynolds Number
U	[m/s]	Inlet Cell Entrance Velocity
V_{trap}	[m^3]	Trap Volume
w	[m]	Particulate Layer Thickness
w_s	[m]	Monolith Wall Thickness
α	[m]	Monolith Cell Size
β	[-]	Forchheimer Coefficient in porous wall
ε	[-]	Monolith Porosity
μ	[kg/ms]	Exhaust Gas Dynamic Viscosity
ν	[m^2/s]	Kinematic Viscosity of Exhaust Gas
ρ	[kg/m^3]	Exhaust Gas Density
ρ_{soot}	[kg/m^3]	Soot Density
σ	[-]	Cell Density
ζ	[-]	Contraction/expansion inertial losses coefficient

PRESSURE DROP MODELS

The back pressure caused by the DPF in the exhaust system is one of the most important parameters that need to be analysed during the design of the filter. Large back pressures have a negative impact on the fuel consumption and CO_2 emissions therefore the back pressure need to be kept lower than a specified limit[3][4]. Various models were developed in order to predict the pressure drop generated by a DPF and the way that this back pressure changes as the soot loading increase.

Bisset's [5] initial work on numerical solutions of DPF regeneration behavior (1983) led to the formation of the first model from Konstandopoulos & Johnson (1989). Opris & Johnson (1998) also derived another model which can be said to be one of the main models since most models found in the literature are based either on this model or on the

Konstandopoulos & Johnson's model [3]. Konstandopoulos & Johnson [6] obtained an equation for the total pressure drop formed between the entrance and the exit of the trap:

$$\Delta P = A_1 + A_2\left[\frac{1}{2} + \frac{c_1}{g_1}\left(e^{g^1} - 1\right) + \frac{c_2}{g_2}\left(e^{g^2} - 1\right)\right] + c_1 g_1 + c_2 g_2 \quad (1)$$

Where

$$A_1 = \frac{k}{\alpha w_s}\frac{4L}{\alpha} Re \quad (2)$$

$$A_2 = 4F\frac{k}{\alpha w_s} \quad (3)$$

$$g_1 = A_1 - \sqrt{{A_1}^2 + 2A_2} \quad (4)$$

$$g_2 = A_1 + \sqrt{{A_1}^2 + 2A_2} \quad (5)$$

$$c_1 = -\frac{1}{2} - c_2 \quad (6)$$

$$c_2 = \frac{1}{2}\left[\frac{e^{g^1}+1}{e^{g^2}+e^{g^1}}\right] \quad (7)$$

In this equation, A_1 and A_2 are functions of trap geometry and flow parameters, g_1 and g_2 are the roots of the characteristic equation of the problem while c_1 and c_2 are constants that are determined from the boundary conditions. [6]

Opris & Johnson [7] proposed a different relation for the pressure drop across the filter. This relationship takes into account the effect of the particulate layer formation inside the filter channels. The pressure drop of a clean filter depends only on the geometry of the filter and exhaust gas properties. As the filter is loaded, particulate matter start to deposit inside the walls and also form a layer on the walls. This changes the properties of the filter walls and therefore affects the total pressure drop across the filter. Particulate layer thickness, permeability and density of the particulate layer are the main properties that affect the pressure drop therefore these are included in the pressure drop equation (equation 8). The pressure drop relation across the filter is:

$$\Delta P = \frac{6\mu LQ}{N(\alpha-2w)^4}\left\{\frac{2(e^{\gamma}+1)+\gamma(e^{\gamma}-1)}{\gamma(e^{\gamma}-1)}\right\} \quad (8)$$

Where

$$\gamma = \sqrt{\frac{48k_e L^2}{(w_s+w)(\alpha-2w)^4}} \quad (9)$$

$$k_e = \frac{kk_{soot}(w_s+w)}{w_s k_{soot} wk} \quad (10)$$

Konstandopoulos [8] continued to develop the Konstandopoulos & Johnson model [6] to obtain a relation between the total pressure drop and porous and frictional losses along the channel length as shown in figure 1.

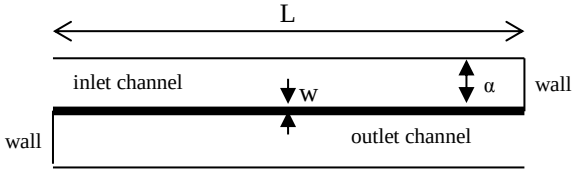

Figure 1 Single channel filter view

The 1-D analytical model of Konstandopoulos & Johnson [6] as shown in Figure1 provides the following relation for a clean filter:

$$\Delta P_{clean} = \frac{\mu}{k}\frac{U\alpha}{4L}w_s + \frac{2\mu F}{3\alpha^2}UL \quad (11)$$

If the trap volume remains constant, the Konstandopoulos & Johnson's model [6] shows that the pressures drop increase with $\left(\frac{L}{D}\right)^{\frac{4}{3}}$. For an optimum pressure drop value, the L/D ratio needs to be kept under unity since the pressure drop value increases exponentially for L/D value above 1. [6] To obtain an optimum value for the cell size (α), the pressure drop equation (3) was modified to include the trap volume (V_{trap}) and the exhaust flow rate (Q).

$$\Delta P = \frac{2\mu Q}{4V_{trap}}\left(1 + \frac{w_s}{\alpha}\right)^2\left\{\frac{\alpha w_s}{k} + \frac{8F}{3}\left(\frac{L}{\alpha}\right)^2\right\} \quad (12)$$

Where

$$V_{trap} = \frac{\pi D^2 L}{4} \quad (13)$$

$$U = \frac{8Q}{\pi D^2 \sigma \alpha^2} \quad (14)$$

Masoudi, Heibel and Then [9] divided the total pressure drop into 4 different pressure drop components. The 4 components making up the total pressure drop are the pressure drop across the filter walls, the pressure drop across the filtration area, the pressure drop caused by flow contraction and expansion effects and finally the pressure drop across the plugs.

The pressure drop caused by the filtration area is taken from the Konstandopoulos & Johnson model [6] pressure drop equation. As shown in Figure 2, exhaust gases contract and expand at the filter inlet and outlet thus contributing to the overall pressure drop. The contraction/expansion inertial loss coefficient is determined empirically. Figure 2 also shows that the filter plugs are too short to allow a fully developed flow to form and thus contribute to the overall pressure drop. The most significant pressure drop component is the pressure drop caused by the exhaust gases flowing through the filter walls. This pressure drop component is divided into two components. For the first component, Darcy's law is used to determine the pressure drop caused by the exhaust gases flowing through the filter walls. The second component is the Forchheimer extension that is used to calculate the pressure drop caused by the inertia effects at high wall-flow velocities. This is due to the fact that at high wall-flow velocities, a non-linear relationship occurs between the pressure drop and the velocity of the exhaust gases.

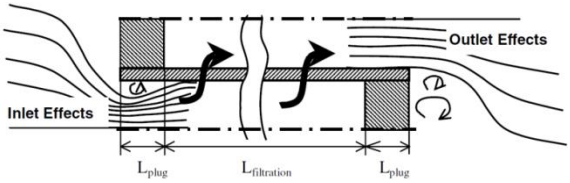

Figure 2 Flow pattern in a clean filter [9]

$$\Delta P_{filtration\ area} = \frac{\mu U d_h w_s}{4Lk}\left[A_1 + A_2\left[\frac{1}{2} + \frac{c_1}{g_1}\left(e^{g^1} - 1\right) + \frac{c_2}{g_2}\left(e^{g^2} - 1\right)\right] + c_1 g_1 + c_2 g_2\right] \quad (15)$$

$$\Delta P_{cont/exp} = \varsigma \frac{\rho}{2} U^2 \quad (16)$$

$$\Delta P_{plug} = Fr \frac{\mu 2 L_{plug} U}{{d_h}^2} \quad (17)$$

$$\Delta P_{wall} = \frac{\mu w_s}{k} U + \beta \rho w_s U^2 \quad (18)$$

$$\Delta P_{total} = \Delta P_{filtration\ area} + \Delta P_{cont/exp} + \Delta P_{plug} + \Delta P_{wall} \quad (19)$$

Konstandopoulos *et al.* [10] extended the Konstandopoulos & Johnson's model [6] for high particulate loading by adding the pressure drop caused by the particulate layer formed in the channel to the pressure drop of a clean filter (equation 20). The clean filter pressure drop equation (equation 11) was modified to represent the pressure drop caused by the filter wall, inlet and outlet channel separately (equation 21).

$$\Delta P_{total} = \Delta P_{filter\ wall} + \Delta P_{soot\ layer} + \Delta P_{inlet\ channel} + \Delta P_{outlet\ channel} \quad (20)$$

$$\Delta P_{clean} = \frac{\mu Q}{2V_{trap}}(\alpha + w_s)^2\left[\frac{w_s}{k\alpha} + \frac{4FL^2}{3\alpha^4} + \frac{4FL^2}{3\alpha^4}\right] \quad (21)$$

To add the particulate layer effects in the clean filter pressure drop equation, the inlet channel part of the equation is modified. The outlet channel and the wall part of the equation remain the same since the particulate layer will only form in the inlet channel. It is assumed that the particulate layer formation is uniform across the filter channel, as shown in figure 3, so that the effective channel width is α-2w and the soot thickness is w. The total pressure drop equation becomes as shown in equation 23.

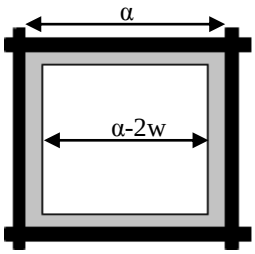

Figure 3 Cross Sectional View of a Loaded Filter

$$w = \frac{\alpha - \sqrt{\alpha^2 - \frac{m_{soot}}{NL\rho_{soot}}}}{2} \quad (22)$$

$$\Delta P = \frac{\mu Q}{2V_{trap}}(\alpha + w_s)^2\left[\frac{w_s}{k\alpha} + \frac{1}{2k_{soot}} ln\left(\frac{\alpha}{\alpha - 2w}\right) + \frac{4FL^2}{3}\left(\frac{1}{(\alpha - 2w)^4} + \frac{1}{\alpha^4}\right)\right] \quad (23)$$

Konstandopoulos *et al.* [13] added the Forchheimer inertial losses to the filter pressure drop equation obtained from Darcy's law as shown in equation (24). The first term of the equation is Darcy's law at low wall velocities while the second quadratic term takes account of the inertial losses.

$$\Delta P = \frac{\mu}{k} U w_s + \beta \rho U^2 w_s \quad (24)$$

The Forchheimer losses β are very difficult to measure experimentally since they occur only at high flow velocities where other inertial contributions may become significant and so the experimental values for β cannot be obtained. [11] Konstandopoulos *et al.* obtained a relation between the Forchheimer coefficient and the permeability of the porous medium as shown in equation (25).

$$\beta = \frac{1.75}{\varepsilon^{\frac{3}{2}}\sqrt{150k}} \quad (25)$$

This relation shows that β is dependent on the porosity and permeability of the filter material. The Forchheimer losses are not significant for a wall flow DPF and so they can be treated as an addition to the clean filter pressure drop equation as shown in equation (26).

$$\Delta P = \frac{\mu Q}{2V_{trap}}(\alpha + w_s)^2\left[\frac{w_s}{k\alpha} + \frac{8FL^2}{3\alpha^4}\right] + \frac{\beta \rho Q^2 (\alpha + w_s)^4 w_s}{4{V_{trap}}^2 \alpha^2} \quad (26)$$

Konstandopoulos *et al.* [12] also added these Forchheimer effects and contraction/expansion inertial losses to the total pressure drop equation, equation (23) that includes the soot loading of the filter as shown in equation (27).

$$\Delta P = \frac{\mu Q}{2V_{trap}}(\alpha + w_s)^2\left[\frac{w_s}{k\alpha} + \frac{1}{2k_{soot}} ln\left(\frac{\alpha}{\alpha - 2w}\right) + \frac{4FL^2}{3}\left(\frac{1}{(\alpha - 2w)^4} + \frac{1}{\alpha^4}\right)\right] + \frac{\rho Q^2 (\alpha + w_s)^4}{{V_{trap}}^2 \alpha^2}\left[\frac{\beta w_s}{4} + 2\zeta\left(\frac{L}{\alpha}\right)^2\right] \quad (27)$$

Nagar *et al.* [11] proposed that the pressure drop across the filter is a sum of the pressure drop due to the exhaust gases flowing through the filter walls, pressure drop due to the frictional losses along the filter channels and the pressure drop caused by the exhaust gas flowing through the particulate layer as shown in equation (28).

$$\Delta P_{total} = \Delta P_{friction} + \Delta P_{walls} + \Delta P_{particulate\ layer} \quad (28)$$

Where

$$\Delta P_{friction} = \frac{\nu U K_f L}{3(\alpha - w_s)^2} + \frac{\nu U K_f L}{3(\alpha - w_s - 2d_{hs})^2} \quad (29)$$

$$\Delta P_{walls} = \frac{\nu U w_s (\alpha - w_s)}{4Lk} \quad (30)$$

$$\Delta P_{particulate\ layer} = \frac{\nu U (\alpha - w_s)^2}{8Lk_{soot}} ln\left(\frac{\alpha - w_s}{\alpha - w_s - 2d_{hs}}\right) \quad (31)$$

EVALUATION OF PRESSURE MODELS

The pressure drop model equations discussed in the previous section were evaluated using the parameters mentioned in table 1. In equations (27), (23), (28), (8) and (19), the pressure drop varies with the soot thickness formed inside the DPF channels and therefore a plot was constructed to show how different soot thickness changes the pressure drop for different models. In the case of equations (11), (12) and (26), the equations do not include a term for soot thickness formation inside the DPF channels therefore a single value can be obtained at clean DPF condition only.

Figure 4 shows that equations (23) and (27), almost overlaps since (27) is a Forchheimer effects extension to equation (23). Equation (28) gives a plot which resembles equations (23) and (27) in shape but its maximum value varies by a quarter. Equation (8) has a very steep gradient and gives high pressure drop values as soot thickness increases. Equation (19) varies very slightly as the soot thickness increases. Equations for a clean DPF (11), (12) and (26) give almost the same value for the pressure drop.

Table 1 Parameters for pressure drop models

Variables& Constants	Unit	Value
Engine size	cm^3	1463
Engine speed	rpm	1000
Air volume rate (intake)	m^3/s	0.01219
Intake air density (15˚C)	kg/m^3	1.225
Mass flow rate (intake)	kg/s	0.01493
R gas constant for exhaust	Nm/kgK	300
Exhaust gases temp.	K	423
Pressure at exhaust exit	Pa	100000
Air volume rate (exit)	m^3/s	0.01895
Exhaust velocity at DPF	m/s	2.8557
Diameter of DPF	m	0.13
Length of DPF	m	0.19
DPF cross sectional area	m^2	0.01327
Volume of DPF trap	m^3	0.00085
DPF wall thickness	m	0.0004
DPF channel sides	m	0.0016
Number of cells	N/A	1754
Air dynamic viscosity	kg/ms	2.2748×10^{-5}
Equivalence ratio ϕ	N/A	0.5
Exhaust dynamic viscosity	kg/ms	2.2445×10^{-5}
Wall permeability	m^2	5.3×10^{-13}
Soot layer Permeability	m^2	3.2×10^{-14}
Factor F	N/A	28.454
Exhaust gas density	kg/m^3	0.83
Porosity of ceramic	%	0.475
Diameter of exhaust pipe	m	0.0762
Contraction/expansion inertial losses coefficient	N/A	0.43089
Forchheimer Coefficient	N/A	599534
Soot density	kg/m^3	650
Exhaust kinematic viscosity (150˚C)	m^2/s	2.9×10^{-5}

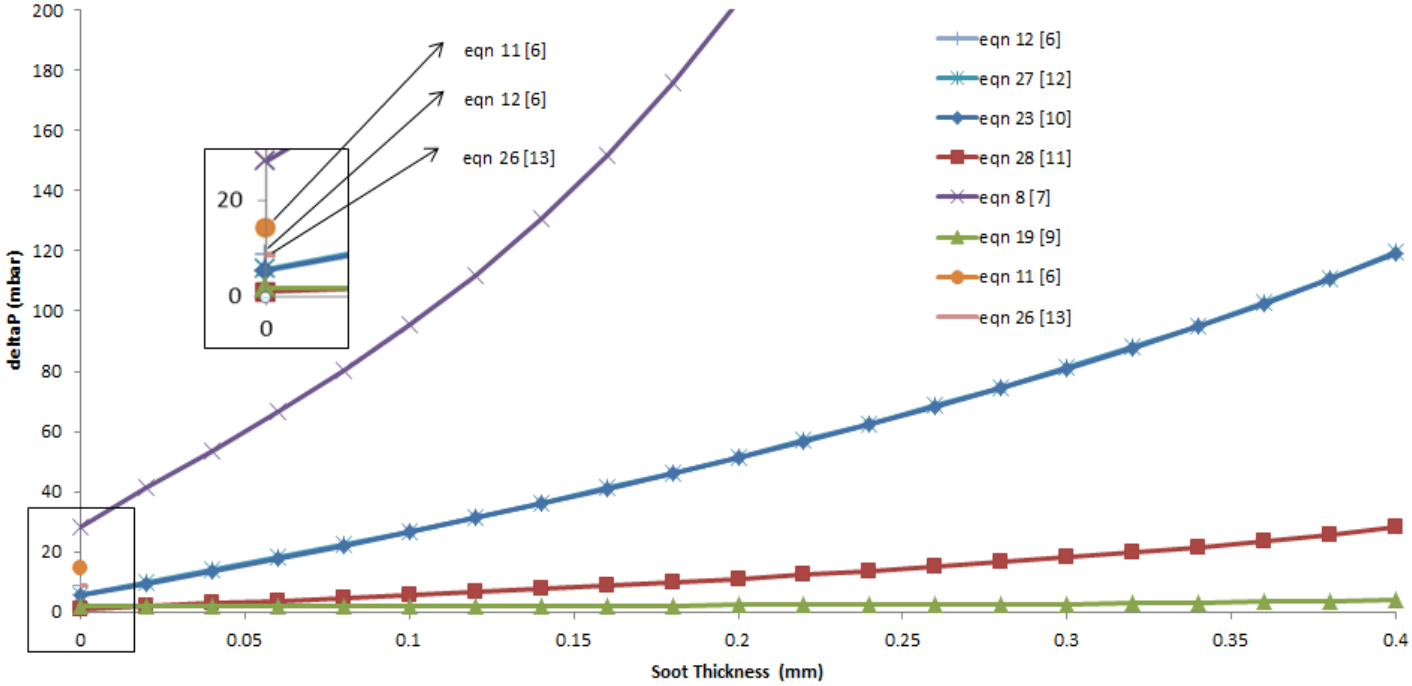

Figure 4 Plot of the pressure drop models vs soot thickness

DPF HEAT PROCEDURE

A totally blocked DPF that was obtained from a Nissan Qashqai was used for this heat procedure with the aim of simulating regeneration process temperatures in order to clean the DPF from accumulated soot.

To reach these temperatures, a furnace consuming 3kW electrical power was used. The temperature inside the furnace was controlled with an Omega CN 4800 temperature controller using a K-type thermocouple. The temperature controller was connected to a contactor which turns on and off the filaments to keep the desired temperatures inside the furnace.[14]

For this procedure, the DPF was cut from the DOC unit so that the heat procedure is performed only on the DPF and also to have a visual assessment of the DPF entrance. A jig was built in order to mark each position of the DPF so it can be accurately rewelded after the procedure is completed. After the DPF was cut from the unit, it was weighed so that a value of removed soot and ash can be determined. The DPF was placed in a vertical position in the furnace so that the soot and ash residues could drop to the furnace bottom. The heating procedure was carried out at different temperatures as shown in table 2. [14]

Table 2 DPF Heat Procedure Temperatures

Temperature	Time Duration	Temperature Gradient
Ramp to 200˚C	20 minutes	10˚C/min
Ramp to 400˚C	40 minutes	5˚C/min
Soak at 400˚C	60 minutes	0˚C/min
Ramp to 550˚C	75 minutes	2˚C/min
Soak at 550˚C	120 minutes	0˚C/min

DPF AIR MASS FLOW MEASUREMENT

A quantitative value of degree of blockage and air resistance that the soot and ash deposits caus was required in order to determine whether the DPF heat procedure was successful. This was obtained by measuring the pressure difference across the DPF and mass flow rates upstream and downstream the DPF before and after the regeneration.

An air blower was used to blow air through the DPF, which was connected using pipes having length more than 10 times the diameter for a fully developed flow. A manometer was used for pressure measurements from a Pitot tube. The blower mass flow rate was measured to make sure it can blow air at mass flow rates equal to a 1.5L engine. This was achieved by measuring the difference between the stagnation and static pressure inside the pipe using equation (32). The maximum air velocity inside the pipe, as shown in equation (33), was calculated from the different in pressures in equation (32). The average air velocity and mass flow rate were then calculated using equations (34) and (35) respectively.

$$P_{dynamic} = \rho_{water} g h_{manometer} \quad (32)$$

$$U_{max} = \sqrt{\frac{2P_{dynamic}}{\rho_{air}}} \quad (33)$$

$$U_{avg} = 0.817 U_{max} \quad (34)$$

$$\dot{m} = \rho_{air} A U_{avg} \quad (35)$$

The air blower was capable of blowing air at a mass flow rate of 121.4g/s which is much more than 38.8g/s that a 1.5L engine blows it exhaust gases.

After each heat treatment the mass flow rates upstream and downstream of the DPF were measured using equations (32) to (35). To obtain the quantitative value of degree of blockage, discharge coefficient (C_d) and blockage factor (K) were also calculated using equations (36) and (37).

$$C_D = \frac{\dot{m}}{A_T P_o \frac{1}{(RT_o)^{\frac{1}{2}}} \left(\frac{P_T}{P_o}\right)^{\frac{1}{\gamma}} \left(\frac{2\gamma}{\gamma-1}\left[1-\left(\frac{P_T}{P_o}\right)^{\frac{\gamma-1}{\gamma}}\right]\right)^{\frac{1}{2}}} \quad (36)$$

$$K = \frac{\Delta P}{\left(\frac{1}{2}\rho_{air} v^2\right)} \quad (37)$$

RESULTS & ANALYSIS

Before the test heat cleaning procedure was initiated, the pressure difference across the DPF was measured and the DPF was also weighed. During the heat cleaning procedure a kilowatt hour (kWh) meter was used on the supply of the furnace to measure the cost of the procedure. It showed that the heat cleaning procedure consumed 8.3kWh of electricity.

After the first heat cleaning procedure was completed, the DPF was shaken to remove solid soot and ash particles that were trapped in the honeycomb structure, and then weighed. The pressure drop across the DPF and the mass flow rates were measured to obtain the values for C_d and K. After the second heat cleaning procedure, the same procedure was performed. The measurements taken before the first heat cleaning procedure and after both heat cleaning procedures are tabulated in table 3 and table 4.

Table 3 Changing Parameters throughout the Procedure

	Before Heat Procedure	After 1st Heat Procedure	After 2nd Heat Procedure
Pressure Difference (kPa)	2.766	1.844	1.296
Discharge Coefficient (C_d)	N/A	0.030422	0.081946
Blockage Coefficient (K)	N/A	10.8818	5.2254
DPF Weight (g)	4083	3744	3719

Table 4 Air Velocity and Mass Flow Rate changing throughout the Procedure

	1st Heat Treatment	2nd Heat Treatment
Average Air Velocity (m/s)	16.095	19.570
Average Mass Flow Rate (g/s)	33.915	41.435

As a result of the process, the pressure drop decreased by more than half from 2.766kPa to 1.296kPa showing that the DPF was successfully regenerated in the furnace. The air velocity and mass flow rate indicate that more air is passing through the filter and therefore it is less restrictive to the flow of air. This is also evident from the discharge coefficient and blockage coefficient values. These values showed that larger flows of air are passing through the filter after the heat treatment was performed and also show that the filter was less restrictive to the flow of air. The weight was also reduced by 364g, the majority of these were released as Carbon Dioxide gas as the soot inside the filter oxidised.

The accumulated mixture of soot and ash that was deposited on the furnace bottom was collected for further analysis, weighing 40g from the total of 364g removed from the DPF. 1g of this mixture was exposed to a temperature of 600˚C in a muffle furnace to measure the amount mixture remaining in the crucible. This was repeated using the same mass but at different time intervals to obtain a relation between percentage weight reduction and time. It was concluded that 1.5 hours were sufficient to oxidise all the soot present in the mixture and have ash particles deposits in the crucible. This procedure was also used to determine the amount of ash found in the DPF. From a total of 364g removed from the DPF, 324g of soot were oxidised and released as CO_2 while from the 40g removed as soot and ash mixture, it was concluded that it contained 10% ash content. This concludes that the ash content of the total 364g removed was only 1%.

CONCLUSION

The two main models discussed previously, the Konstandopoulos & Johnson's model and the Opris & Johnson's model, gave very similar pressure drop values when plotted against the changing soot thickness. As other losses and effects occurring inside the DPF are added to these basic equations, the values vary by a significant difference. Konstandopoulos *et al.* extensions increased the values by more than 10 times the basic model at high soot loading.

The heat cleaning procedure performed was successful in oxidising a large portion of the accumulated soot in the totally blocked DPF and bringing back the DPF into its original state. This conclusion was supported by the measurements taken to obtain a quantitative value of the degree of blockage. The method used was a relatively cheap method and no consumables were used during this process. The ash content was determined to be very low, 1% of the soot.

REFERENCES

[1] http://ec.europa.eu/environment/air/transport/road.htm

[2] Zhan, R., Huang, Y., and Khair, M., Methodologies to control DPF uncontrolled regenerations, *SAE World Congress Detroit,* Michigan, Paper number 2006-01-1090, 3-6 April, 2006.

[3] Charbonnel, S., and Opris, C.N., Fundamental Diesel Filter (DPF) Pressure Drop Model, *SAE International,* Paper number 2009-01-1271

[4] Masoudi, M,. Konstandopoulos, A.G., Nikitidis, M.S., Skaperdas, E., Zarvalis, D., Kladopoulou, E., and Altiparmakis, C., Validation of a Model and Development of a Simulator for Predicting the Pressure Drop, *SAE World Congress Detroit,* Michigan, Paper number 2001-01-0911, 5-8 March, 2001.

[5] Bissett, E.J., Mathematical Model of the Thermal Regeneration of a wall-flow monolith Diesel Particulate Filter, *Chemical Engineering Science, USA,* Vol. 39, 1984, pp.1233-1244

[6] Konstandopoulos A.G., and Johnson, J.H., Wall-Flow Diesel Particulate Filters- Their Pressure Drop and Collection Efficiency, *SAE Technical Paper,* Paper number 890405

[7] Opris C.N., and Johnson J.H A 2-D Computational Model Describing the Flow and Filtration Characteristics of a Ceramic Diesel Particulate Trap, *SAE International Congress and Exposition Detroit,* Michigan, Paper number 980545, 23-26 February, 1998.

[8] Konstandopoulos, A.G., Skaperdas, E., Warren, J., and Allansson, R., Optimized Filter Design and Selection Criteria for Continuously Regenerating Diesel Particulate Traps, *SAE International Congress and Exposition Detroit,* Michigan, Paper number 1999-01-0468, 1-4 March, 1999.

[9] Masoudi, M., Heibel, A., and Then, P., Predicting Pressure Drop of Wall-Flow Diesel Particulate Filters – Theory and Experiment, *SAE World Congress Detroit,* Michigan, Paper number 2000-01-0184, 6-9 March, 2000.

[10] Konstandopoulos, A.G., Kostoglou, M., Skaperdas, E., Papaioannou, E., Zarvalis, D., and Kladopoulou, E., Fundamental Studies of Diesel Particulate Filters: Transient Loading, Regeneration and Aging, *SAE World Congress Detroit,* Michigan, Paper number 2000-01-1016, 6-9 March, 2000.

[11] Nagar, N., He, X., Iyengar, V., Acharya, N., and Kalinowski, A., Real Time Implementation of DOC-DPF Models on a Production-Intent ECU for Controls and Diagnostics of a PM Emission Control System, *SAE Int. Commer. Veh* Volume 2, Issue 2, Paper number 2009-01-2904

[12]Konstandopoulos, A.G., Skaperdas, E., and Masoudi, M., Microstructural Properties of Soot Deposits in Diesel Particulate Traps, *SAE World Congress Detroit,* Michigan, Paper number 2002-01-1015, 4-7 March, 2002

[13]Konstandopoulos, A.G., Skaperdas, E., and Masoudi, M., Inertial Contributions to the Pressure Drop of Diesel Particulate Filters, *SAE World Congress Detroit,* Michigan, Paper number 2001-01-0909, 5-8 March, 2001

[14] Xuereb, E., Analysis of Diesel Particulate Filter Blockage Problem in Malta and Heat Cleaning Procedure, *Bachelor of Engineering (Hons.) of University of Malta Dissertation,* May 2015

ACKNOWLEDGMENTS

The technical assistance by Andrew Briffa of the Thermodynamics Laboratory was vital in this work. The financial support of The University of Malta Research Fund and Endeavour scholarship scheme is also acknowledged.